ACS APPLIED MATERIALS & INTERFACES

Research Article

www.acsami.org

Surface Functionalization of Zirconium Phosphate Nanoplatelets for the Design of Polymer Fillers

Brian M. Mosby, Agustín Díaz, Vladimir Bakhmutov, and Abraham Clearfield*

Department of Chemistry, Texas A&M University, P.O. Box 30012, College Station, Texas 77842, United States

Supporting Information

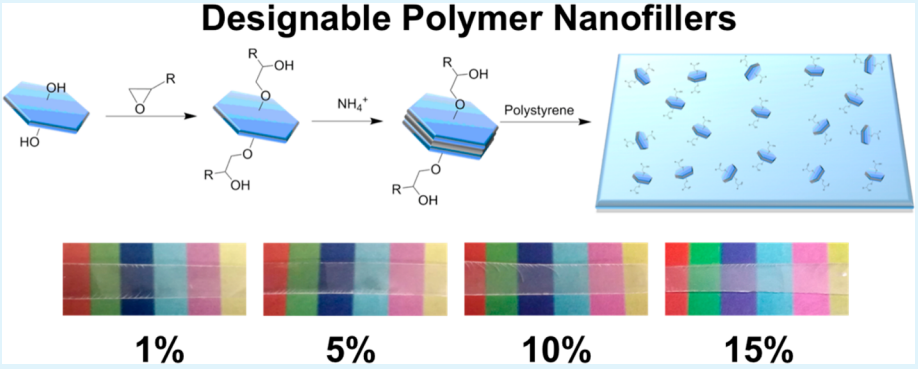

ABSTRACT: Inorganic−organic hybrid materials were synthesized by covalent attachment of epoxides to the surface of zirconium phosphate (ZrP) nanoplatelets. X-ray powder diffraction, FTIR, and TGA were utilized to confirm the presence of the modifiers and exclusive functionalization of the ZrP surface. NMR experiments were conducted to confirm the formation of P−O−C bonds between surface phosphate groups and epoxide rings. The applicability of the organically modified products was demonstrated by their use as fillers in a polymer matrix. Subsequently, a two step intercalation and surface modification procedure was utilized to prepare polymer nanocomposites that were imparted with functionality through the encapsulation of molecules within the interlayer of surface modified ZrP.

KEYWORDS: *surface modification, tetravalent metal phosphates, self-assembled monolayers, inorganic layered materials, polymer nanocomposites*

INTRODUCTION

Self-assembled monolayers (SAMs) have attracted much attention over the past three decades due to the simplicity of synthesis and broad range of applicability. Netzer and Sagiv originally found that reaction of trichlorosilanes with the hydroxyl terminated surface of SiO_2 led to addition of a monolayer, which greatly altered the properties of the material.[1] The smooth faces of silicon based platforms with Si−H and Si−OH bonds made them the initial platforms of choice; subsequently, SAMs have extended to a large number of platforms including gold and metal oxides.[2,3] SAMs are of interest due to the ability of the monolayer to alter the properties of the material. By carefully choosing the substrate and composition of the monolayer, SAMs have found applicability in a large number of fields such as chemical sensors, biosensors, cell adhesion, microelectronics, and thin film technology.[4,5] The principles of SAMs were soon applied to nanoparticles in which case surface modification is used to build monolayers. As is the case with SAMs, modification of nanoparticles can alter the properties of the material and dictate how they interact with their environment.

Metal phosphates make up one of the largest families of inorganic layered materials. α-Zirconium hydrogen phosphate ($Zr(O_3POH)_2{\cdot}H_2O$, ZrP) is one of these materials, which has been extensively studied since being reported by Clearfield and Stynes in 1964.[6] Single crystal X-ray diffraction data of the α phase showed that the Zr atoms lie in a plane, slightly below and above the layer, and are connected to each other by phosphate groups. Three of the oxygen atoms of each phosphate group are bonded to a different Zr atom, and the remaining hydroxyl group points away from the layer, either in the interlayer region or on the surface.[7] The arrangement of the layers forms a zeolitic cavity where a water molecule resides; this cavity has been utilized for intercalation chemistry, the reversible incorporation of guest molecules into the interlayer, and has given ZrP a large range of applications ranging from drug delivery to nanocomposites.[8−12]

The introduction of organic functionality into ZrP was thought to be ideal as a means of producing hybrid materials with diverse applicability. Alberti found that organic derivatives of ZrP could be achieved by reaction of zirconium fluoro complexes with phosphonic acids or phosphoric acid esters.[13]

Received: October 21, 2013
Accepted: December 6, 2013
Published: December 6, 2013

 © 2013 American Chemical Society

In these organic derivatives the interlayer and surface of the compound contain the R group, thus incorporating the organic directly into the structure. Eventually it was found that organic derivatives could be achieved post synthetically. Yamanaka and Ortiz-Avila and Clearfield reported the bonding of ethylene oxide with γ- and α-ZrP, respectively, by esterification of the P−OH groups.[14,15] More recently, Pica et al. reported the complete modification of α-ZrP using 1,2-epoxydodecane as the coupling agent and exfoliated α-ZrP as the precursor in a tetrahydrofuran (THF) suspension as well as the functionalization of ZrP through exchange of the phosphate groups with phosphonic acids.[16,17] In our own efforts we were able to modify α-ZrP with octadecylisocyanate, forming a hydrophobic monolayer on the surface of the platelets.[18] The isocyanate group not only reacts with the surface but also with the edges of the platelets. When the modified ZrP was exfoliated it produced a mixture of Janus and Gemini nanoplatelets that were used as stabilizers in Pickering emulsions.[18] In addition, we have also reported the surface modification of α-zirconium phosphate nanoparticles, previously loaded with tris(2,2′-bypiridyl) ruthenium(II), with octadecyltrichlorosilane producing highly hydrophobic nanoparticles which were used in a photoinduced electron transfer reaction in a non-polar solvent.[19]

These results clearly indicate that the P−OH groups of α-ZrP are indeed reactive. Although the intercalation chemistry of the interlayer region has been heavily investigated, ZrP also has an interesting and unique surface chemistry, which has been largely ignored. The flat surface of ZrP would be an ideal platform for reactivity, as it is expected that the disorder of alkyl modifiers that results from the nanoscopic curvature of silica surfaces will not persist in the case of ZrP.[20] In addition, manipulation of both the interlayer and surface of ZrP could lead to development of new classes of materials with tunable properties and could also greatly improve the applicability of all the current ZrP based systems. Herein we describe the exclusive surface functionalization of ZrP with epoxides, 2-(4-fluorophenyl) oxirane, styrene oxide, 1,2-epoxy-9-decene, 1,2-epoxydodecane, and 1,2-epoxyoctadecane. The modified particles were then utilized to prepare novel polymer nanocompoites in which functionality was added to the composite by exploiting the intercalation chemistry of ZrP.

EXPERIMENTAL SECTION

Materials. Zirconyl chloride octahydrate (98%, $ZrOCl_2{\cdot}8H_2O$), polystyrene (MW ~ 192 000), 1,2-epoxydodecane (90%, $C_{12}H_{24}O$), and 2-(4-fluorophenyl)-oxirane (95%, C_6H_7FO) were purchased from Sigma-Aldrich; 1,2-epoxy-9-decene (96%, $C_{10}H_{18}O$), 1,2-epoxyoctadecane (90%, $C_{18}H_{36}O$), and styrene oxide (98+%, C_8H_8O) were purchased from Alfa Aesar; and ammonium hydroxide solution (~14.8 M, NH_4OH) and phosphoric acid (85%, H_3PO_4) were purchased from EMD Chemicals. All chemicals were used as purchased, without further purification.

Synthesis of α-ZrP. α-ZrP was synthesized using the reflux method described by Sun with minor modifications adapted from Kijima.[21,22] A total of 3.22 g of $ZrOCl_2{\cdot}8H_2O$ was dissolved in 200 mL of water and added dropwise to 200 mL of 6 M H_3PO_4 at 94 °C. The mixture was kept under reflux for 48 h. Upon completion of the reaction the product was rinsed with deionized water, centrifuged three times at 3000 rpm, and dried in an oven at 65 °C overnight.

Surface Modification of ZrP with Epoxides. A total of 100 mg of α-ZrP was placed in a 50 mL round bottom flask followed by addition of 25 mL of toluene. A stoichiometric amount of epoxide (5:1) was then added followed by sonication of the vessel. The vessel was refluxed at 111 °C for 12 h while stirring. In all cases the reaction products were washed multiple times with hexanes and ethanol, filtered, and dried in an oven at 65 °C.

Synthesis of SO/NH_4^+@ZrP. In a typical experiment, 0.500 g of SO/ZrP was dispersed in 300 mL of solvent and ammonium was intercalated based upon the method of Clearfield and co-workers.[23] In this case a stoichiometric amount of NH_4OH solution was added drop-wise to the dispersed nanoparticles, after which the solution was allowed to stir for two additional hours. The solution was centrifuged and dried in an oven at 65 °C to recover the product.

Preparation of Polystyrene (PS)−Styrene Oxide/ZrP (SO/ZrP) Nanocomposites. PS−SO/ZrP nanocomposites were prepared using the following method. Initially, 1 g of polystyrene was dissolved in 10 mL of toluene. Enough styrene oxide ZrP (SO/ZrP) to reach the desired loading percent was then dispersed in 10 mL of toluene and added to the original polystyrene solution. The mixture was then sonicated until well-dispersed, and excess solvent was removed by rotary evaporation. The resulting viscous solution was then poured into an aluminum pan, dried in a vacuum desiccator, and then placed in an oven overnight at 85 °C. The films were then allowed to cool at room temperature until hardened. The same procedure was used to prepare PS composites with SO/NH_4^+@ZrP.

Characterization of Modified ZrP. Surface modification of ZrP was confirmed by a combination of techniques. The interlayer spacing was confirmed by X-ray powder diffraction (XRPD), FTIR was used to identify the presence of the modifier through their vibration modes, and thermogravimetric analysis was carried out to determine the amount of modifier bonded to the ZrP platform. More detailed information was obtained by solid state NMR. XRPD experiments were performed from 2 to 40° (2θ-angle) using a Bruker-AXS D8 short arm diffractometer equipped with a multi-wire lynx eye detector using Cu Kα (λ = 1.542 Å) and operated at a potential of 40 kV and a current of 40 mA. Thermogravimetry experiments were carried out on a TGA Q500 TA Instrument. Samples were heated from room temperature to 800 °C at a heating rate of 5 °C per minute under a mixture of air and N_2 (9:1). The $^{31}P\{^1H\}$ and $^{13}C\{^1H\}$ MAS NMR experiments were performed with a Bruker Avance-400 spectrometer (400 MHz for ^1H nuclei) using a standard 7-mm MAS probe head at a spinning rate of 6 kHz. Standard one pulse (direct nuclear excitation) and/or CP pulse sequences were applied in these experiments at relaxation delays necessary for a quantitative analysis of the spectra. The contact times of 2 and 6 ms were adjusted for ^{13}C and ^{31}P nuclei in the CP experiments. The external standards used for ^{13}C and ^{31}P NMR experiments were TMS and H_3PO_4 solution, respectively. The transmission electron micrographs (TEM) of the samples were acquired using a JEOL 2010 transmission electron microscope at an acceleration voltage of 200 kV. FTIR spectra were acquired using a Bruker Tensor 37 Fourier Transform Infrared Spectrophotometer in ATR (attenuated total reflection) mode with a ZnSe crystal. Measurements were taken from 600 to 4000 cm^{-1} at a resolution of 4.0 cm^{-1}, and 32 scans were averaged. UV−visible measurements were obtained using a Shimadzu UV-1601PC spectrophotometer.

RESULTS AND DISCUSSION

Nanocrystal Morphology before and after Surface Modification. The XRPD patterns of both α-ZrP and epoxide modified ZrP samples are provided in Figure 1A. The first peak in the α-ZrP pattern shows a d-spacing of 7.6 Å. This spacing corresponds to the interlayer distance between the 002 planes of α-ZrP. It is expected that if the surface of the material has been successfully modified that this distance should remain unchanged. An increase in this spacing would indicate that the modifier reacted with the interlayer region or intercalated within the layers, which in this case is unwanted. Examination of Figure 1A shows that all the XRPD patterns display a d-spacing of 7.6 Å. The identical interlayer distances suggest there is no unwanted interaction of the epoxide with the interlayer; therefore, any modification that occurred must be exclusively on the surface of the nanoplatelets. Although the 002 peak is in

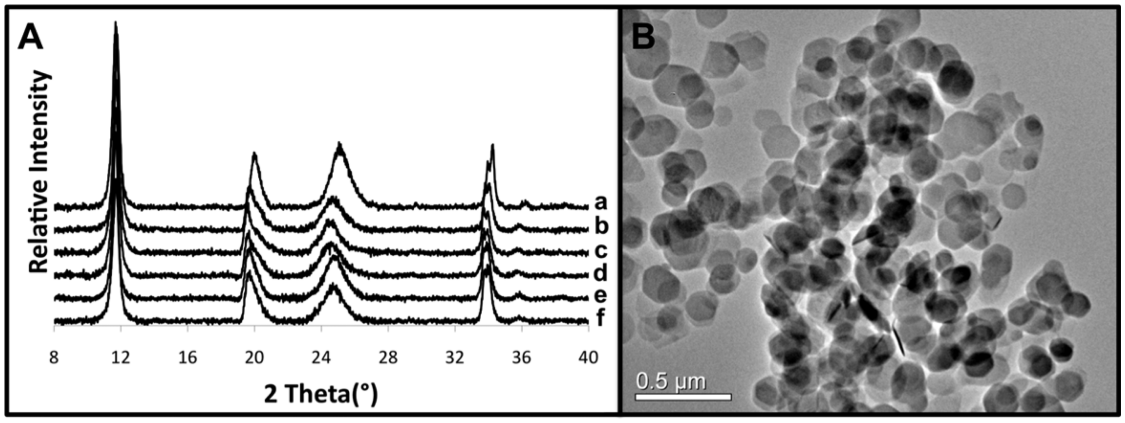

Figure 1. (A) XRPD patterns of ZrP and modified samples showing that the modification does not affect the interlayer spacing. (a) α-ZrP, (b) 1,2-epoxyoctadecane/ZrP, (c) 1,2-epoxydodecane/ZrP, (d) 1,2-epoxy-9-decene/ZrP, (e) styrene oxide/ZrP, and (f) fluorophenyl oxirane/ZrP. (B) TEM image of 1,2-epoxyoctadecane/ZrP displaying the retention of the nanocrystal morphology after modification.

the same position it can be observed from the pattern that the subsequent peaks are shifted to lower 2θ values when compared to pristine ZrP. The shift observed is indicative of dehydration of ZrP; several studies have shown that upon dehydration the hydrogen bonding with the interlayer water is lost and a new hydrogen bonding interaction is formed with other phosphate groups producing a more rigid structure.[24,25] The fact that the 002 peaks are identical, while the subsequent peaks are shifted, suggests that the particles are only partially dehydrated. It is well known that the thermal behavior of ZrP is contingent upon the crystallinity of the material, where less crystalline samples lose the interlayer water more readily than samples of higher crystallinity.[26−28] In previous investigations it was found that crystalline ZrP can be completely dehydrated by prolonged heating at 110 °C.[28] In addition, the continued reflux of ZrP in phosphoric acid has also been shown to yield dehydrated phases of ZrP.[24] As the surface modification was conducted at 111 °C in this case, and the particles are of low crystallinity, the observed dehydration is reasonable. TEM images of epoxide modified particles, Figure 1B, further confirm that the particle shape and crystallinity are not affected by the surface reaction and are nearly identical to that of pristine ZrP (Figure SI-1, Supporting Information). The average particle size of the functionalized particles is 120 nm, which is in the expected range for particles prepared by reflux methods with 3 M H_3PO_4 according to Sun et al.[21] The thickness of the particles observed by electron microscopy is ca. 8.5 nm (Figure SI-2, Supporting Information), which agrees well with previous studies.[11,19]

Fourier Transform Infrared Spectroscopy (FTIR). The surface modification products were then analyzed by FTIR to determine if any of the epoxide modifiers were successfully bonded to the surface. The IR of α-ZrP is comprised mainly of stretches due to the phosphate groups and the lattice water; a detailed discussion is given by Horsley.[29] In summary the stretches at 3590 cm^{-1}, 3510 cm^{-1}, 3150 cm^{-1}, and 1618 cm^{-1} are all from the stretching and bending of the lattice water, and the large range of stretching frequencies is seen due to the two crystallographically of different phosphates in ZrP hydrogen bonding to different extents with the interlayer water molecule. The infrared spectra of the epoxide modified ZrP shows a mixture of vibration modes for the epoxide and the ZrP, where the ZrP dominates the spectrum due to the high concentration of ZrP layers relative to the modifiers on the top and bottom surfaces, Figure 2. The expected region for C−H stretching

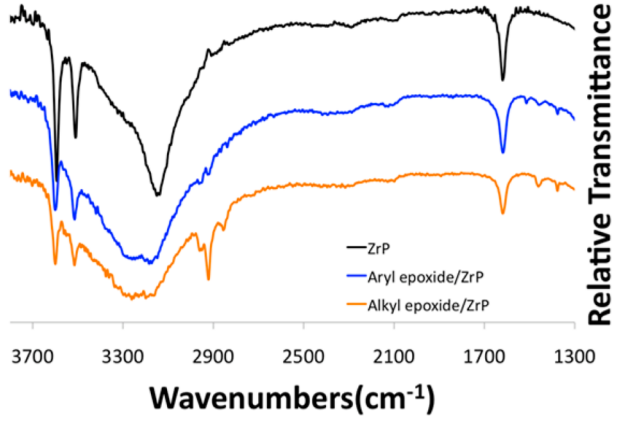

Figure 2. FTIR spectra of epoxide modified ZrP, along with a typical example of aryl epoxide modified ZrP (fluorophenyl oxirane/ZrP) and alkyl epoxide (1,2-epoxydodecane/ZrP) modified ZrP focusing on the region where stretches due to modification appear.

between 2850 cm^{-1} and 3000 cm^{-1} can be seen for all ZrP modified with alkyl epoxides, and stretches can also be observed between 1350 cm^{-1} and 1480 cm^{-1} due to C−H bending. Aryl epoxides display stretches at 690 cm^{-1}, 710 cm^{-1}, and 1500 cm^{-1} for the arene functionality. In all cases a signal appears at 910 cm^{-1} for the phosphate ester (Figure SI-3, Supporting Information), which is a result of the covalent attachment of the epoxide to the surface phosphate group.

In addition, the stretches for the lattice water are still present, confirming that there is no interaction of the modifier with the interlayer region or intercalation. Upon successful intercalation of a molecule in the interlayer region of ZrP the stretches for the water in the zeolitic cavities no longer exist due to the exchange of the interlayer water with the intercalated molecule. Although the water stretch is present it is slightly deformed due to the partial dehydration of the surface modified product, as discussed earlier (vide infra). These results combined with the XRPD supports exclusive esterification of the ZrP surface. On the other hand, it has been established that FTIR can be used to identify the degree of disorder of aliphatic chains on nanoparticle surfaces.[20] It has been reported that crystalline microenvironments are formed when long alkyl chain lengths greater than six carbon atoms are assembled on oxidized surfaces.[30] Disordered systems (liquid-like) show a CH_2

dx.doi.org/10.1021/am4046553 | ACS Appl. Mater. Interfaces 2014, 6, 585−592

asymmetric stretching band near 2924 cm^{-1}, while with more ordered monolayers the band appears closer to 2917 cm^{-1}, indicating a more crystalline state. In our case the asymmetric stretching appears at ~2924 cm^{-1} for the 1,2-epoxydodecane (C_{12}) alkyl chain and at 2922 cm^{-1} for the 1,2-epoxy-9-decene (C_{10}) and 1,2-epoxyoctadecane (C_{18}) chains. It was expected that the C_{18} chain would be more ordered than the shorter chains, and the fact that the C_{10} shows identical ordering as the C_{18} is likely due to π interactions of the terminal alkene functionality of the C_{10} chains.

Thermogravimetric Analysis (TGA). To quantify the amount of modifier on the surface of the ZrP nanoparticles, thermogravimetric analysis (TGA) was used. The total weight loss of α-ZrP is ~12%, with two major weight losses wherein the sample is completely dehydrated and the phosphate groups condense to yield zirconium pyrophosphate as the end product [$Zr(O_3POH)_2{\cdot}H_2O(s)$ + heat (700 °C) → $2H_2O(g)$ + $ZrP_2O_7(s)$].[31] The weight loss of the modified samples occurs in three events as is seen for similar organically modified ZrP materials.[16,18,19] All surface and interlayer water and residual solvent is expected to be lost below 150 °C. The next weight loss occurring anywhere from 200 °C to 350 °C is expected to be the loss of the organic modifier. Lastly, the condensation of the monohydrogenphosphate to the pyrophosphate occurs roughly between 450 °C and 600 °C; typical thermograms can be seen in Figure 3. The percent weight losses obtained are all

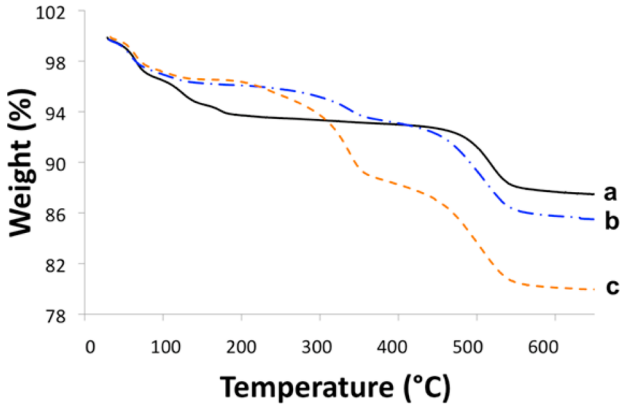

Figure 3. TGA of α-ZrP along with aryl and alkyl modified samples. (a) α-ZrP, (b) styrene oxide/ZrP, and (c) 1,2-epoxyoctadecane/ZrP.

within the expected range. Using the TGA results, formulas and molecular weights of the surface modified samples can be obtained; this information is presented in Table 1.

Surface Coverage. It has now been confirmed that the epoxide groups have been successfully attached to the ZrP surface. A theoretical mass contribution can be calculated for a sample in which all surface phosphates have been successfully modified by taking into account the nanoparticle thickness, number of reactive surface sites, and one to one interaction of epoxide rings with surface phosphate groups. A proportion of the mass contribution observed in the TGA with the theoretical value yields an estimate of the surface coverage. The simplest approximation is as follows. Initially, the number of inorganic layers present in the nanoparticle is calculated by dividing the thickness of the particle by the interlayer distance. In our case the nanoparticles were found to be ca. 8.5 nm, and the interlayer distance of ZrP is 7.6 Å (0.76 nm); therefore, we estimate about 11 layers per nanoparticle. A mass contribution of the layers can be obtained by multiplying the number of layers by the molecular weight of ZrP. To estimate the contribution of the organic modifier the molecular weight of the epoxide is multiplied by two as only the top and bottom layers will be modified. A ratio of the mass contributions of the organic modifier to ZrP yields an estimate for the percent weight loss, corresponding to the epoxide, which should be observed in the TGA of a surface modified material if all sites are covered.

The percent coverage estimates are collected in Table 1 along with the TGA data and calculated formulas. All estimates range from 60% to 87%, and the moles of epoxide are all within the same general vicinity. This suggests that sterics do not play a major role in the bonding of the epoxides, which is reasonable as each surface phosphate group is 5.28 Å apart.[32]

Solid State Nuclear Magnetic Resonance (SSNMR). To further investigate the bonding within the surface modified particles both ^{31}P and ^{13}C SSNMR experiments were carried out. All epoxide reactions proceed through bonding of the surface phosphate groups with the epoxide rings; therefore, the ^{31}P-NMR spectra should be similar with similar surface coverage regardless of which epoxide is used (Figure SI-4, Supporting Information). In the case of 1,2-epoxyoctadecane/ZrP, the ^{31}P spectrum reveals four signals of which two can be assigned to ZrP, Figure 4. The most dominant signal of the spectrum at ca. −19 ppm is assigned to the orthophosphate group of ZrP. The orthophosphate group consists of a phosphorus atom, which is bonded to three Zr atoms through three oxygen atoms. On the basis of structural studies, this is the prevalent phosphorus in ZrP; therefore, it is expected to give rise to an intense signal. The weak resonance at −17.1 ppm is also characteristic of ZrP. The literature nearly always assigns the ^{31}P spectra of α-ZrP as a single peak; however, close examination of published spectra shows a slight shoulder on the left of the dominant peak, which is not mentioned or assigned in many cases (Figure SI-5, Supporting Information).[33−38] This small peak is prevalent in materials that are less crystalline and prepared through reflux methods. It is possible that during washing of the material that the expected 2:1 P:Zr ratio is reduced by hydrolysis of the phosphates and leaves a small percentage of phosphate in a different environment from the bulk, especially on the edges of the particles.[39] The remaining

Table 1. Summary of TGA Data along with Estimated Percent Coverage (assuming 11 layers) and Proposed Formulas for Epoxide Modified ZrP

modifier	total TGA weight loss (%)	percent coverage (%)	calculated formula
fluorophenyl oxirane	17.24	87.3	$Zr(H_{0.831}PO_4)_2(Mod)_{0.169}{\cdot}0.7H_2O$
styrene oxide	14.65	67.6	$Zr(H_{0.873}PO_4)_2(Mod)_{0.127}{\cdot}0.6H_2O$
1,2-epoxy-9-decene	15.22	62.2	$Zr(H_{0.882}PO_4)_2(Mod)_{0.118}{\cdot}0.5H_2O$
1,2-epoxydodecane	17.15	72.5	$Zr(H_{0.860}PO_4)_2(Mod)_{0.140}{\cdot}0.6H_2O$
1,2-epoxyoctadecane	20.18	69.4	$Zr(H_{0.861}PO_4)_2(Mod)_{0.139}{\cdot}0.6H_2O$

dx.doi.org/10.1021/am4046553 | ACS Appl. Mater. Interfaces 2014, 6, 585−592

signals are observed at −21.4 and −22.4 ppm. The signal at −21 ppm can be assigned to the dehydrated phase of ZrP and is in good agreement with the XRD, IR, and TGA data, which suggests a lower level of hydration than pristine ZrP.[35] It is likely that during the extended reflux some of the interlayer water that was held loosely escaped the interlayer. The second signal can be assigned to the phosphorus atom that has been esterified and is involved in modification through a P−O−C linkage, as previously reported by Pica et al.[16]

In addition to the observation of successful modification in the ^{31}P NMR, bonding of the alkyl chains to the surface of the samples agrees well with the CP/MAS ^{13}C-NMR spectra of 1,2-epoxyoctadecane/ZrP. In the case of epoxides, for each bond to the surface only two distinct carbons appear; there should be a P−O−C linkage to the surface and also the C−OH that occurs as a result of the ring-opening of the epoxide. The signals for the alkyl carbons are observed from 10.4 ppm to 30.4 ppm, and additional signals pertaining to the ring-opening of the epoxide are present at 63 ppm, 69.9 ppm, and 77.8 ppm. These resonances can be assigned to carbon environments that are a direct result of covalent attachment of epoxide to the ZrP surface. Previous reports suggest that epoxides can adopt two bonding formations, one in which a secondary alcohol is formed, which is the dominant product, and the other in which a primary alcohol is formed.[16] In the former case signals at ∼62 ppm are assigned to the P−O−C linkage and signals at ∼71 ppm are assigned to the carbon atom of the secondary alcohol. In the latter case it is thought that the P−O−C linkage is seen at the same place as the previous case, but the carbon atom of the primary alcohol is thought to be observed at ∼80 ppm. There are some slight shifts in the values from the surface modified samples as opposed to those reported for the fully functionalized derivative, but they are indeed indicative of the same carbon environments. It should also be noted that the signals of the three membered ring of the starting organic material are absent in the spectra; this confirms that all organic matter present is covalently attached to the ZrP platform.

As expected our results greatly differ from those obtained by Pica et al.[16] In our synthesis we focus on exclusively functionalizing the surface, whereas Pica attempted to functionalize all P−OH groups homogenously throughout the material. In regards to the ^{31}P spectra, Pica was able to identify three distinct signals at −22.6 ppm, −24.7 ppm, and −19 ppm that corresponded to the two different epoxide bonding conformations and the free P−OH groups, respectively. The epoxide bonding confirmations made up 99.5% of the integral, whereas free P−OH made up 0.5%. Integration in our material leads to 19% epoxide bonding confirmations and 81% that corresponded to the base ZrP structure, in good agreement with our surface coverage estimation. The ^{13}C spectra are largely identical; however, the signals indicative of ring-opening of the epoxide are much less intense in our spectra due to the fact that we are functionalizing only the surface P−OH groups. The fact that unmodified phosphates dominate our ^{31}P spectra while the presence of the reactive epoxide can be confirmed by CP/MAS ^{13}C-NMR greatly supports the exclusive functionalization of the nanoplatelet surface.

Polymer Nanocomposites. As the surface group can be varied to have alkyl or aryl functionality, it is expected that these materials can be designed for use as fillers in a variety of polymers to improve compatibility between the organic and inorganic components. ZrP has been used in the past for inorganic fillers in polymers, but most approaches involved

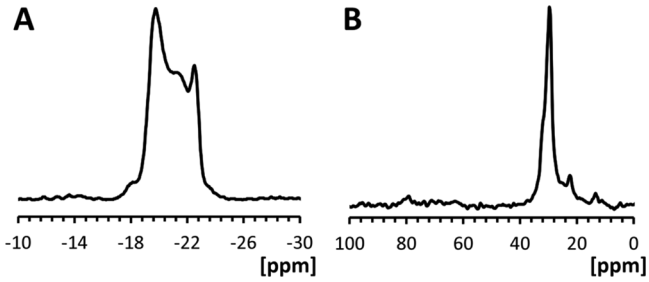

Figure 4. MAS solid state NMR of 1,2-epoxyoctadecane/ZrP. (A) ^{31}P{^{1}H}, (B) ^{13}C CP.

exfoliation to disperse individual nanosheets throughout the polymer, intercalation of the monomer within the layers of ZrP followed by polymerization, synthesis of an organic derivative of ZrP to make the particles compatible with the polymer, or direct synthesis of ZrP inside ionic polymers by addition of phosphoric acid to a Zr(IV) exchanged polymer.[10,17,40−46] Although this approach is an organic derivative, it is novel as α-ZrP can be dispersed within the polymer without delamination of the layers and without changing the interlayer functionality. This allows for the unique opportunity to add specific functionality to the composite by intercalation into ZrP before it is dispersed in the polymer. The following is demonstrated with polystyrene and SO/ZrP loaded with ammonium ions (SO/NH_4^+@ZrP) as a potential fire resistant polymer nanocomposite.

Two phases are possible when intercalating ammonium ions into ZrP, the fully loaded phase in which there are 2 moles of ammonium ion per Zr, and the half loaded phase which has a 1:1 ratio of Zr:NH_4^+.[23,47] Composites were successfully prepared for the fully loaded phase, and the effect of the encapsulated molecule on the thermal stability of the nanocomposites was investigated. Initially the composite films were analyzed by XRPD. The PS film is amorphous and yields no diffraction other than the halo observed as a result of the sample holder (ca. 16−25° 2θ); therefore, all peaks present in the powder pattern are a result of the SO/NH_4^+@ZrP dispersed within the polymer matrix. It can be observed in Figure 5 that as the percentage loading of SO/NH_4^+@ZrP increases the diffraction of the films increases. In all cases diffraction was observed from the film that was indicative of the corresponding ammonium intercalated ZrP phase, and thus verifies that the particles remain intact and are not delaminated. The first peak that occurs shows a *d*-spacing of 9.03 Å, which is

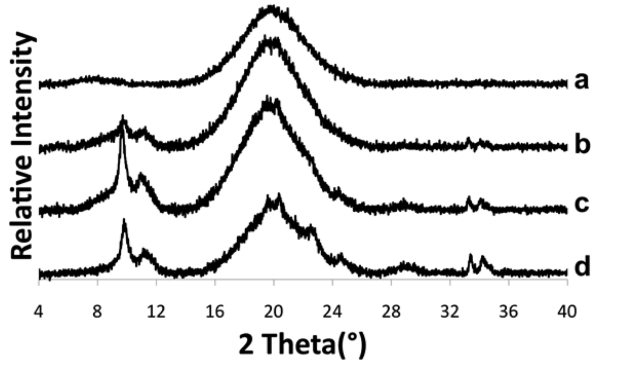

Figure 5. XRPD patterns of SO/NH_4^+@ZrP composite films of various loadings (% w/w). (a) 1%, (b) 5%, (c) 10%, and (d) 15%.

dx.doi.org/10.1021/am4046553 | ACS Appl. Mater. Interfaces 2014, 6, 585−592

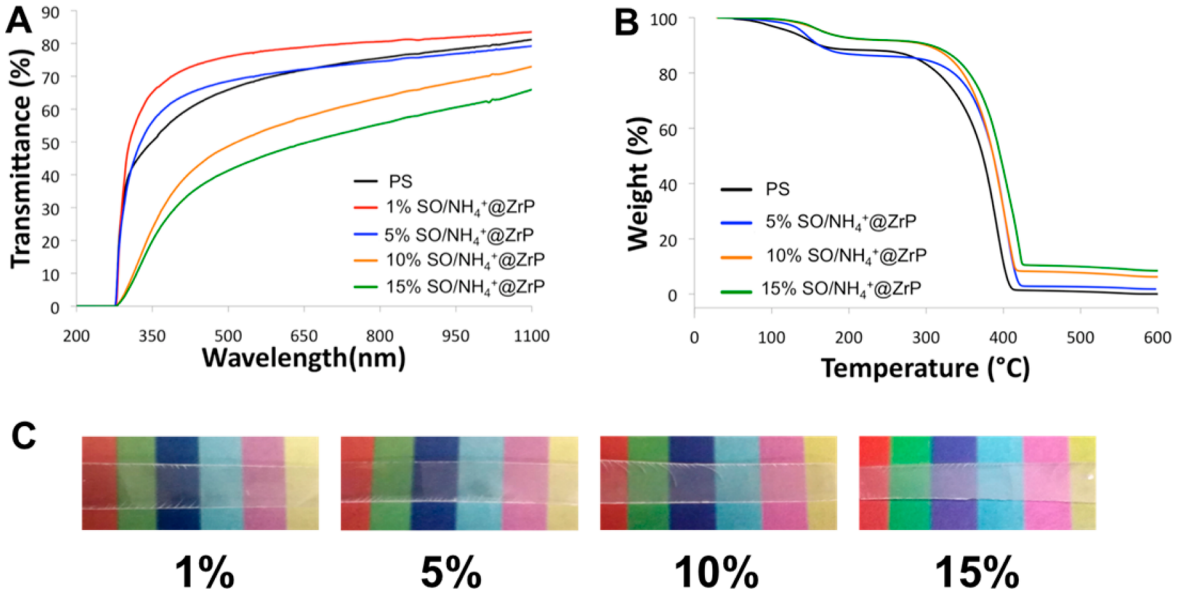

Figure 6. (A) UV−visible spectra of the composite films showing the transparency of the composites at various nanofiller loadings. (B) TGA data of PS composite with SO/ammonium ZrP displaying the delay in weight loss and increases thermal decomposition temperature, and (C) image of the composite films displaying the transparency of the composites.

a result of the intercalation of ammonium ion into the nanoplatelets. This peak is followed by a broad peak centered at a 2θ value of ca. 11°. This peak is likely a combination of two peaks with d values of 8.2 Å and 7.6 Å which were reported by Hasegawa and Aoki as the initial indication of the re-exchange of protons into NH_4^+@ZrP.[47] The intercalation of ammonium within ZrP is highly ionic in nature, each ammonium is surrounded by the maximum number of negative charges and the water molecules positioning is based upon the location of the ammonium.[23] It is likely that upon heating the motion of water molecules could have caused reorganization within the layer facilitating the production of the new phases. Other diffraction peaks of the SO/NH_4^+@ZrP starting material are also observed at 2θ values between 20° and 25° and at ca. 34°. Ultimately the signals observed are slightly shifted when compared to the SO/NH_4^+@ZrP particles themselves (Figure SI-6, Supporting Information); this is likely due to instrumental effects as one sample was analyzed in powder form and the other as a film.

Both the transparency and thermal stability of the nanocomposites was then investigated (Figure 6 A-C). All composites appear to be transparent; however, UV−visible spectroscopy was utilized to investigate the level of transparency, Figure 6A. Composites with nanoparticle loadings of 5% and below were shown to retain the transparency of the original PS film whereas a decrease in transparency was observed for loadings of 10% and above. The decreased transparency and red shift observed in the onset of the spectra can be attributed to aggregation of nanoparticles within the polymer.[48,49] Overall, the nanoparticles are dispersed somewhat uniformly in the polymer, but some aggregation is likely to occur at higher loading levels. TGA was utilized to study the thermal stability of the nanocomposite and the influence of the intercalated guest into the nanofillers on the thermal stability, Figure 6B. The derivative of the thermograms reveals three weight loss events. The first event ranging roughly from 110 °C to 170 °C can be attributed to the toluene that is incorporated in the film due to strong interactions with the polystyrene and the water in the interlayer of ZrP. The second decomposition is that of the polymer and occurs anywhere between 360 °C and 411 °C for polystyrene but fluctuates depending on the loading of the ZrP (Table 2). Lastly, from 500 °C to 550 °C the condensation of ZrP to zirconium pyrophosphate can be observed verifying that the particles were not delaminated and that the full particle was dispersed in the composite. In all cases it is observed that the intercalated composites are more stable than PS and the SO/ZrP composites, and not only is the thermal decomposition delayed but the temperature at which the decomposition ends is increased due to the presence of the nanofillers (Figure SI-7, Supporting Information). This suggests that the presence of NH_4^+ in the composite adds thermal stability. The results demonstrate that it is possible to add functionality into composites through intercalation of a surface modified nanoparticle without hindering the thermal stability of the composite; in this case the stability was improved upon. Utilizing this approach, numerous combinations of surface groups and intercalated molecules can be utilized to make nanocomposites for particular applications. This technique and these customized nanocomposites will be investigated further in a future publication.

Table 2. Thermal Analysis Data for SO/NH_4^+@ZrP Composites

loading (% w/w)	ΔT_{Max} (°C)	temperature at ΔT_{Max} (°C)	final decomposition temperature (°C)
0%	--	--	414
1%	4.8	252	414
5%	18.6	396	425
10%	19.6	396	425
15%	30.8	402	430

CONCLUSIONS

In conclusion, we have shown that it is possible to selectively functionalize the surface of zirconium phosphate nanoparticles with epoxides to synthesize inorganic−organic hybrid materials.

dx.doi.org/10.1021/am4046553 | ACS Appl. Mater. Interfaces 2014, 6, 585−592

This functionalization leads to new organic derivatives of ZrP in which the top and bottom layers are modified while the interlayer structure remains unchanged. This is the first known report of an epoxide functionalized inorganic layered material in which the interlayer is unaffected and is still available to perform intercalation or ion exchange chemistry. These materials were then used as fillers in polymers and it was demonstrated that nanoparticles that are surface modified and intercalated with some molecule could be used to add specific functionality to polymer composites. Tailoring the surface groups of ZrP could greatly enhance the potential applicability of ZrP and improve upon all current applications of the material.

■ ASSOCIATED CONTENT

Supporting Information

Additional characterization of materials including TEM and ^{31}P NMR of the ZrP starting material, TEM, FTIR, and ^{31}P NMR of epoxide modified samples, and powder XRD and thermal data on polymer composite. This information is available free of charge via the Internet at http://pubs.acs.org/.

■ AUTHOR INFORMATION

Corresponding Author

*Fax: 979-845-2370. Tel.: 979-845-2936. E-mail: clearfield@chem.tamu.edu.

Notes

The authors declare no competing financial interest.

■ ACKNOWLEDGMENTS

This work was supported by the Texas A&M University Graduate Diversity Fellowship (B.M.M.), the Robert A. Welch Foundation Grant A-0673, and the National Science Foundation Grant DMR-0652166, for which grateful acknowledgement is made. We would like to acknowledge the Microscopy and Imaging Center and X-ray Diffraction Laboratory at Texas A&M University for the use of the TEM and XRPD facilities.

■ ABBREVIATIONS

ZrP, zirconium phosphate; FTIR, Fourier transform infrared spectroscopy; TGA, thermogravimmetric analysis; XRPD, X-ray powder diffraction; NMR, nuclear magnetic resonance; PS, polystyrene; NH_4^+@ZrP, ammonium loaded ZrP

■ REFERENCES

(1) Netzer, L.; Sagiv, J. *J. Am. Chem. Soc.* **1983**, *105*, 674−676.
(2) Ulman, A. *Chem. Rev.* **1996**, *96*, 1533−1554.
(3) Love, J. C.; Estroff, L. A.; Kriebel, J. K.; Nuzzo, R. G.; Whitesides, G. M. *Chem. Rev.* **2005**, *105*, 1103−1170.
(4) Flink, S.; van Veggel, F. C. J. M.; Reinhoudt, D. N. *Adv. Mater.* **2000**, *12*, 1315−1328.
(5) Kumar, A.; Biebuyck, H. A.; Whitesides, G. M. *Langmuir* **1994**, *10*, 1498−1511.
(6) Clearfield, A.; Stynes, J. A. *J. Inorg. Nucl. Chem.* **1964**, *26*, 117−129.
(7) Troup, J. M.; Clearfield, A. *Inorg. Chem.* **1977**, *16*, 3311−3314.
(8) Díaz, A.; Saxena, V.; Gonzalez, J.; David, A.; Casanas, B.; Carpenter, C.; Batteas, J. D.; Colon, J. L.; Clearfield, A.; Delwar Hussain, M. *Chem. Commun.* **2012**, *48*, 1754−1756.
(9) Wu, H.; Liu, C.; Chen, J.; Yang, Y.; Chen, Y. *Polym. Int.* **2010**, *59*, 923−930.
(10) Casciola, M.; Bagnasco, G.; Donnadio, A.; Micoli, L.; Pica, M.; Sganappa, M.; Turco, M. *Fuel Cells* **2009**, *9*, 394−400.
(11) Saxena, V.; Diaz, A.; Clearfield, A.; Batteas, J. D.; Hussain, M. D. *Nanoscale* **2013**, *5*, 2328−2336.
(12) Guevara, J. S.; Mejia, A. F.; Shuai, M.; Chang, Y.-W.; Mannan, M. S.; Cheng, Z. *Soft Matter* **2013**, *9*, 1327−1336.
(13) Alberti, G.; Costantino, U.; Allulli, S.; Tomassini, N. *J. Inorg. Nucl. Chem.* **1978**, *40*, 1113−1117.
(14) Yamanaka, S. *Inorg. Chem.* **1976**, *15*, 2811−2817.
(15) Ortiz-Avila, C. Y.; Clearfield, A. *Inorg. Chem.* **1985**, *24*, 1773−1778.
(16) Casciola, M.; Capitani, D.; Donnadio, A.; Munari, G.; Pica, M. *Inorg. Chem.* **2010**, *49*, 3329−3336.
(17) Pica, M.; Donnadio, A.; Troni, E.; Capitani, D.; Casciola, M. *Inorg. Chem.* **2013**, *52*, 7680−7687.
(18) Mejia, A. F.; Diaz, A.; Pullela, S.; Chang, Y.-W.; Simonetty, M.; Carpenter, C.; Batteas, J. D.; Mannan, M. S.; Clearfield, A.; Cheng, Z. *Soft Matter* **2012**, *8*, 10245−10253.
(19) Díaz, A.; Mosby, B. M.; Bakhmutov, V. I.; Martí, A. A.; Batteas, J. D.; Clearfield, A. *Chem. Mater.* **2013**, *25*, 723−728.
(20) Jones, R. L.; Pearsall, N. C.; Batteas, J. D. *J. Phys. Chem. C* **2009**, *113*, 4507−4514.
(21) Sun, L.; Boo, W. J.; Sue, H. J.; Clearfield, A. *New J. Chem.* **2007**, *31*, 39−43.
(22) Kijima, T. *Bull. Chem. Soc. Jpn.* **1982**, *55*, 3031−3032.
(23) Clearfield, A.; Troup, J. M. *J. Phys. Chem.* **1973**, *77*, 243−247.
(24) Clearfield, A.; Landis, A. L.; Medina, A. S.; Troup, J. M. *J. Inorg. Nucl. Chem.* **1973**, *35*, 1099−1108.
(25) Krogh Andersen, A. M.; Norby, P.; Hanson, J. C.; Vogt, T. *Inorg. Chem.* **1998**, *37*, 876−881.
(26) Horsley, S. E.; Nowell, D. V. *J. Appl. Chem. Biotechnol.* **1973**, *23*, 215−224.
(27) La Ginestra, A.; Patrono, P. *Mater. Chem. Phys.* **1987**, *17*, 161−179.
(28) Clearfield, A.; Costantino, U. In *Solid-state Supramolecular Chemistry: Two- and Three-dimensional Inorganic Networks*, 1st ed.; Alberti, G., Bein, T., Eds.; Pergamon Press: Oxford, 1996; Vol. 7, pp 111−112.
(29) Horsley, S. E.; Nowell, D. V.; Stewart, D. T. *Spectrochim. Acta* **1974**, *30A*, 535−541.
(30) Sambasivan, S.; Hsieh, S.; Fischer, D. A.; Hsu, S. M. *J. Vac. Sci. Technol. A* **2006**, *24*, 1484−1488.
(31) Clearfield, A.; Pack, S. P. *J. Inorg. Nucl. Chem.* **1975**, *37*, 1283−1290.
(32) Clearfield, A.; Smith, G. D. *Inorg. Chem.* **1969**, *8*, 431−436.
(33) Clayden, N. J. *J. Chem. Soc., Dalton Trans.* **1987**, 1877−1881.
(34) Segawa, K.-i.; Nakajima, Y.; Nakata, S.-i.; Asaoka, S.; Takahashi, H. *J. Catal.* **1986**, *101*, 81−89.
(35) MacLachlan, D. J.; Morgan, K. R. *J. Phys. Chem.* **1990**, *94*, 7656−7661.
(36) Rodriguez-Castellon, E.; Olivera-Pastor, P.; Maireles-Torres, P.; Jimenez-Lopez, A.; Sanz, J.; Fierro, J. L. G. *J. Phys. Chem.* **1995**, *99*, 1491−1497.
(37) Capitani, D.; Casciola, M.; Donnadio, A.; Vivani, R. *Inorg. Chem.* **2010**, *49*, 9409−9415.
(38) Tahara, S.; Takakura, Y.; Sugahara, Y. *Chem. Lett.* **2012**, *41*, 555−557.
(39) Clearfield, A.; Oskarsson, A.; Oskarsson, C. *Ion Exch. Membr.* **1972**, *1*, 91−107.
(40) Boo, W. J.; Sun, L.; Liu, J.; Clearfield, A.; Sue, H.-J. *J. Phys. Chem. C* **2007**, *111*, 10377−10381.
(41) Sun, L.; Boo, W. J.; Sun, D.; Clearfield, A.; Sue, H.-J. *Chem. Mater.* **2007**, *19*, 1749−1754.
(42) Sun, L.; Liu, J.; Kirumakki, S. R.; Schwerdtfeger, E. D.; Howell, R. J.; Al-Bahily, K.; Miller, S. A.; Clearfield, A.; Sue, H.-J. *Chem. Mater.* **2009**, *21*, 1154−1161.
(43) Pica, M.; Donnadio, A.; Bianchi, V.; Fop, S.; Casciola, M. *Carbohydr. Polym.* **2013**, *97*, 210−216.
(44) Casciola, M.; Alberti, G.; Donnadio, A.; Pica, M.; Marmottini, F.; Bottino, A.; Piaggio, P. *J. Mater. Chem.* **2005**, *15*, 4262−4267.

(45) Casciola, M.; Capitani, D.; Comite, A.; Donnadio, A.; Frittella, V.; Pica, M.; Sganappa, M.; Varzi, A. *Fuel Cells* **2008**, *8*, 217−224.
(46) Sue, H. J.; Gam, K. T.; Bestaoui, N.; Spurr, N.; Clearfield, A. *Chem. Mater.* **2003**, *16*, 242−249.
(47) Hasegawa, Y.; Aoki, H. *Bull. Chem. Soc. Jpn.* **1973**, *46*, 836−838.
(48) Xiong, H.-M.; Zhao, X.; Chen, J.-S. *J. Phys. Chem. B* **2001**, *105*, 10169−10174.
(49) Singhal, A.; Dubey, K. A.; Bhardwaj, Y. K.; Jain, D.; Choudhury, S.; Tyagi, A. K. *RSC Adv.* **2013**, *3*, 20913−20921.